I J C T A, 10(5) 2017, pp. 701-712

Power Quality Improvement by using Fuzzy Logic Controller for SHPF and TCR

M. Sai Gopinath*, **V. Joshi Manohar****, **P. Pandarinath***** and **Saida Rao******

Abstract: Now a days in any industrial and domestic applications large power electronic equipments are increasingly used. When discussing about power electronics equipment's having the lot of parameters are need to consider like harmonic contamination, disturbances of non-linear loads, and fluctuations of output voltages and currents etc. so in this concept the combination of shunt and TCR active filters are used as a compensate the voltage and current mitigate any form of voltage and current fluctuations and power factor correction in a power distribution network. When used as a fuzzy logic controller was adapted control the TCR. For current trailing and voltage regulation a nonlinear control of APF was developed. The latter is based mostly on a decoupled control strategy that considers that the controlled system could be divided into an inner quick loop and an outer slow one. Thus, an actual linearization management was applied to the inner loop, and a nonlinear feedback control law was used for the outer voltage loop. Integral compensators were added in each current and voltage loops in order to eliminate the steady-state errors due to system parameter uncertainty. MATLAB SIMULINK environment has been used to validate the proposed techniques and comparative analysis have been carried out.

Keywords: Hybrid power filter, fuzzy logic controller, Shunt active power filter, thyristor-Controller reactor, %THD.

1. INTRODUCTION

Power system suffers from serious issues of great harmonics currents with poor input power issue caused by nonlinear masses. The line current harmonics cause increase in losses, instability, and additionally voltage distortion. Historically, each passive and active filters are used close to harmonic manufacturing masses or at the purpose of common coupling to dam current harmonics. Shunt filters still dominate the harmonic compensation at medium/high voltage level, whereas active filters are declared for low/medium voltage ratings. Passive filtering has been most popular for harmonic compensation in distribution systems as a result of low price, simplicity, responsible and management less operation. Passive filters are found appropriate with numerous applications involving reactive power at the side of harmonic compensation by thyristor switched filters (TSF) that contains several passive filters and therefore the variation of load power are often adjusted [1]-[2]. The issues of passive filters are often slaked by active filters have an honest performance and more practical in harmonic compensation except for massive scale system the active filter price is high [3]-[11]. The hybrid filter consists of a series connection of a tiny low rated active filter and a fifth-tuned LC passive filter. Within the projected topology, the major part of the compensation is supported by the passive filter and therefore the TCR whereas the APF is supposed to boost the filtering characteristics and damps the resonance, which may occur between the passive filter, the TCR, and therefore the supply resistance. The shunt APF once used alone suffers from the high kV ampere rating of the electrical converter, which needs lot of energy hold on at high dc-link voltage. On the opposite hand, as revealed by some authors [12], the quality hybrid power filter is unable to compensate the reactive power due to the behavior of the passive filter. Hence, the proposed combination of SHPF and TCR compensates for unwanted reactive power and harmonic currents. Additionally, it reduces considerably the Volt ampere rating of the APF half. The control technique of the combined compensator is conferred. An effect technique is projected to

* M.Tech Student, Dept. of EEE, Guntur Engineering College, Guntur, A.P. *Email: sainadh65@gmail.com*
** Professor, Dept. of EEE, Guntru Engineering College, Guntur, A.P. *Email: vjoshimanohar@gmail.com*
*** Professor, Guntur Engineering College, Guntur, A.P. *Email: principalgec@gmail.com*
**** Assistant Professor, Dept. of EEE, Guntur Engineering College, Guntur, A.P. *Email: saidarao4@gmail.com*

boost the dynamic response and reduce the steady-state error of the TCR [13]. It consists of a PI controller and a lookup table to extract the specified firing angle to compensate a reactive power consumed by the load. A nonlinear control of SHPF is developed for current tracking and voltage regulation functions. It's supported a decoupled management strategy that considers that the controlled system is also divided into inner quick loop and an outer slow one [14].

2. SHPF-TCR COMPENSATOR SYSTEM CONFIGURATION

The proposed concept was shown in Figure 1, its combination of SHPF-TCR. The 5th-tuned LC passive filter was connected in series with small-rating of SHPF. The APF has 3-phase full-bridge voltage-source inverter (VSI) with pulse with modulation (PWM) and an input inductor, resistor (L_{pf}, R_{pf}) and bus capacitor (C_{dc}). In power grid using APF with stands very small voltages and currents, and then its rated capacity is significantly reduced. The proposed system implements in power system having advantages like compensating reactive power and eliminating harmonic currents. The shunt passive filter (SPF) is formed by connecting passive filter in parallel mode. With the use of SPF in power system to correct Power factor (PF) and to compensate the 5th harmonic. The small-rating APF is used to eliminate the menace of resonance between the SPF and grid. And it is also used to filter harmonics generated by TCR and the load. The reactive power regulation is achieved by using TCR.

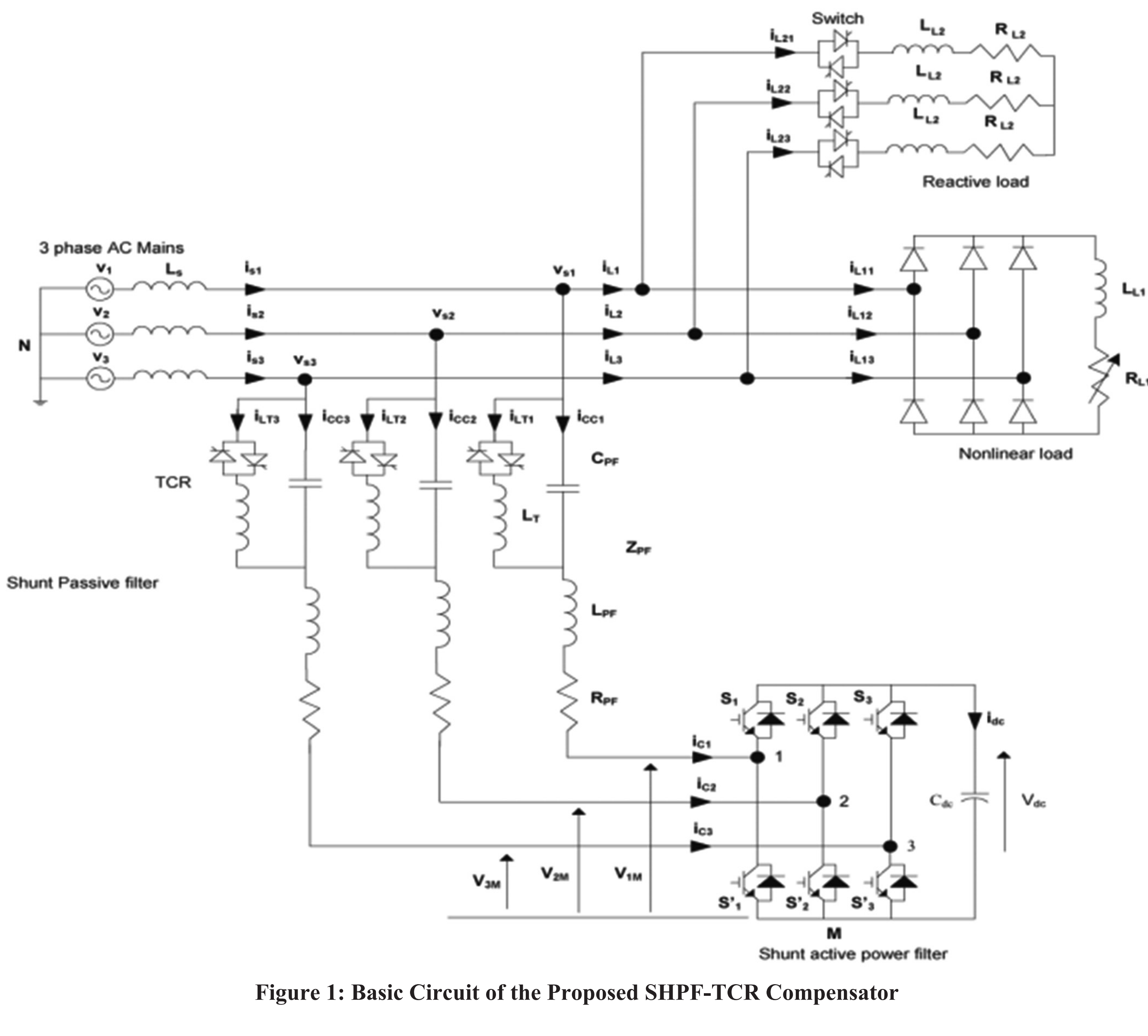

Figure 1: Basic Circuit of the Proposed SHPF-TCR Compensator

3. SHPF-TCR COMPENSATOR CONFIGURATION

A. Thyristor-Controlled Reactor

TCR means Thyristor is connected in anti-parallel with series connected linear air-cored reactor [3]. The main asset of TCR is regulation of reactive power. The thyristor pair which are connected in anti-parallel mode acts like a bidirectional switch, with these switch the Thyristor valveT1&T2 are conducting positive and negative half cycles respectively. The thyristor firing angle is measured from the terminals of the zero crossing voltage.

B. Shunt Hybrid Power Filter

The schematic consists of the supply voltage and diode rectifier. The filtering system contains series connected small rating active power filter with the LC passive filter. The source harmonic compensation improved with hybrid filter by increasing the characteristics of the compensation in passive filter also removing the resonance risk [4]. Effective compensation of current harmonics and limited supply of voltage distortion is provided by SHPF. The harmonic currents of the nonlinear load flow through the passive filter by controlling the hybrid filter. And that the ac mains supplies the fundamental component of the load current.

4. PROPOSED SYSTEM MODELING AND CONTROL

A. Modeling of SHPF

By using Kirchhoff's voltage law, the below equations 1, 2 and 3 are expanded.

$$v_{s1} = \mathrm{L_{PF}}\frac{di_{c1}}{dt} + \mathrm{R_{PF}}i_{c1} + \mathrm{V_{CPF1}} + \mathrm{V_{1M}} + \mathrm{V_{MN}}$$

$$v_{s2} = \mathrm{L_{PF}}\frac{di_{c2}}{dt} + \mathrm{R_{PF}}i_{c2} + \mathrm{V_{CPF2}} + \mathrm{V_{2M}} + \mathrm{V_{MN}}$$

$$v_{s3} = \mathrm{L_{PF}}\frac{di_{c3}}{dt} + \mathrm{R_{PF}}i_{c3} + \mathrm{V_{CPF3}} + \mathrm{V_{3M}} + \mathrm{V_{MN}}$$

$$v_{\mathrm{CPF1}} = \mathrm{L_T}\frac{di_{c1}}{dt} - \mathrm{C_{PF}L_T}\frac{d^2\mathrm{V_{CPF1}}}{dt^2}$$

$$v_{\mathrm{CPF2}} = \mathrm{L_T}\frac{di_{c2}}{dt} - \mathrm{C_{PF}L_T}\frac{d^2\mathrm{V_{CPF2}}}{dt^2}$$

$$v_{\mathrm{CPF3}} = \mathrm{L_T}\frac{di_{c3}}{dt} - \mathrm{C_{PF}L_T}\frac{d^2\mathrm{V_{CPF3}}}{dt^2}$$

$$\frac{d\mathrm{V}_{dc}}{dt} = \frac{1}{\mathrm{C}_{dc}}i_{dc} \tag{1}$$

The k^{Th} leg of converter's switching function c_k is defined as (for $k = 1, 2, 3$)

$$\mathrm{C}_k = \begin{cases} 1, \text{if } \mathrm{S_K} \text{ is on and } \mathrm{S_K}, \text{ is off} \\ 0, \text{if } \mathrm{S_K} \text{ is off and } \mathrm{S_K}, \text{ is on} \end{cases} \tag{2}$$

The state-run function of switching d_{nk} is explained as

$$d_{nk} = \left(c_k - \frac{1}{3} \sum_{m=1}^{3} c_m \right) \tag{3}$$

Furthermore, the following transfer model in 3-phase coordinates is formed by the absence of the zero sequence in the ac voltages, currents and in the $[d_{nk}]$

$$\mathrm{L_{PF}} \frac{di_{c1}}{dt} = -\mathrm{R_{PF}} i_{c1} - d_{n1} v_{dc} - v_{\mathrm{CPF1}} + \mathrm{V_{S1}}$$

$$\mathrm{L_{PF}} \frac{di_{c2}}{dt} = -\mathrm{R_{PF}} i_{c2} - d_{n2} v_{dc} - v_{\mathrm{CPF2}} + \mathrm{V_{S2}}$$

$$\mathrm{L_{PF}} \frac{di_{c3}}{dt} = -\mathrm{R_{PF}} i_{c3} - d_{n3} v_{dc} - v_{\mathrm{CPF3}} + \mathrm{V_{S3}}$$

$$\mathrm{C}_{dc} \frac{d\mathrm{V}_{dc}}{dt} + \frac{\mathrm{V}_{dc}}{\mathrm{R}_{dc}} = d_{n1} i_{c1} + d_{n2} i_{c2} + d_{n3} i_{c3} \tag{4}$$

The system of (4) is transformed into the synchronous orthogonal frame using the following general transformation matrix:

$$\mathrm{C}_{dq}^{123} = \sqrt{\frac{2}{3}} \begin{bmatrix} \cos\theta & \cos\left(\theta - \frac{2\pi}{3}\right) & \cos\left(\theta - \frac{4\pi}{3}\right) \\ -\sin\theta & -\sin\left(\theta - \frac{2\pi}{3}\right) & -\sin\left(\theta - \frac{4\pi}{3}\right) \end{bmatrix} \tag{5}$$

Where $\theta = \omega t$ and the following equalities hold:

$$\mathrm{C}_{123}^{dq} = (\mathrm{C}_{dc}^{123})^{-1} = (\mathrm{C}_{dc}^{123})^{\mathrm{T}} \tag{6}$$

The state space model of the system applying by dq transformation in the synchronous reference frame.

The state space model is nonlinear because it has multiplication terms between the switching state function $\{d_{nd}, d_{nq}\}$. And state variables $\{i_d, i_q, \mathrm{V}_{dc}\}$. Then also the state space model is invariant time during a switching state. Moreover the SHPF operation principle requires that the three variable have to control individually [3]. By effectively separating their respective dynamics to avoid the interaction between the inner loop and the outer dc bus voltage loop.

B. Harmonic Current Control

A slow outer dc voltage loop and fast inner current loop are adapted as show in the Figure 2 the first two equations in the model can be written. There is no significant negative impact on the performance of the proposed control technique [14] of 1st and 2nd derivative TCR capacitor voltages, because the coefficients are too low.

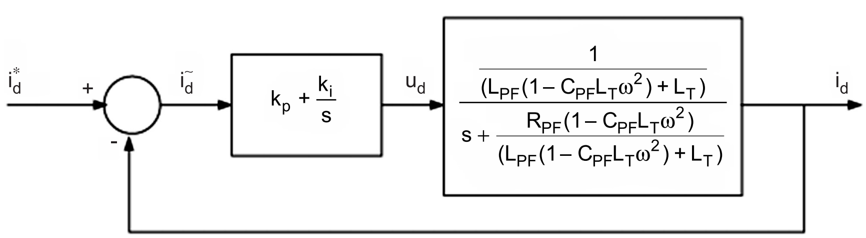

Figure 2: Inner control loop of the current i_d

With the above information the i_d and i_q currents can be controlled independently and the decoupled dynamics of the current tracking is obtained. More over a fast dynamic response and zero study errors can be achieved by using proportional integral compensation. The tracking controller's expressions are

$$u_d = \left(L_{PF}\left(1 - C_{PF}L_T\omega^2\right) + L_T \frac{di_d}{dt} + R_{PF}\left(1 - C_{PF}L_T\omega^2\right)i_d = k_p i_d + k_i \int i_d \, dt \right)$$

$$u_q = \left(L_{PF}\left(1 - C_{PF}L_T\omega^2\right) + L_T \frac{di_q}{dt} + R_{PF}\left(1 - C_{PF}L_T\omega^2\right)i_q = k_p i_q + k_i \int i_q \, dt \right)$$

The proportional-integral controller transfer function is given as

$$G_{i1}(s) = \frac{u_d(s)}{i_d(s)} = k_{p1} + \frac{k_{i1}}{s} \tag{7}$$

$$G_{i2}(s) = \frac{u_d(s)}{i_d(s)} = k_{p2} + \frac{k_{i2}}{s}$$

In Figure 3 the inner control loop of the current i_d is showed. The closed-loop transfer functions of the current loops are

$$\frac{i_d(s)}{i_d^*(s)} = \frac{k_{p1}}{A} \frac{S + \dfrac{K_{i1}}{K_{P1}}}{S^2 + \left(\dfrac{B + K_{P1}}{A}\right)S + K_{i1}}$$

$$\frac{i_d(s)}{i_d^*(s)} = \frac{k_{p2}}{A} \frac{S + \dfrac{K_{i2}}{K_{P2}}}{S^2 + \left(\dfrac{B + K_{P2}}{A}\right)S + K_{i2}} \tag{8}$$

In the following form the current loops, closed loop transfer functions are given,

$$\frac{i_d(s)}{i_d^*(s)} = 2\varepsilon\omega_{ni} \frac{s + \dfrac{\omega_{ni}}{2\varepsilon}}{s^2 + 2\varepsilon\omega_{ni}\, s + \omega_{ni}^2}$$

The above equation ω_{ni} is the outer loop natural angular frequency and ζ is the damping factor. For the optimal value of the damping factor $\zeta = \sqrt{2}/2$, the theoretical overshoot is 20.79%. The following design relations can be derived:

$$k_{p1} = k_{p2} = 2\varepsilon\omega_{ni}(L_{PF}(1 - L_{PF}L_T\omega^2) + L_T) - R_{PF}(1 - C_{PF}L_T\omega^2)$$

$$k_{i1} = k_{i2} = (L_{PF}(1 - C_{PF}L_T\omega^2) + L_T)\omega_{ni}^2 \tag{9}$$

In the Appendix note the control law is given that the inputs q_{nd} and q_{nq} having nonlinearity cancellation part and a linear decoupling compensation part.

C. DC Bus Voltage Regulation

At a desired value, to maintain the dc bus voltage, acting on i_q can compensate the losses through the hybrid power filter [8] components. To the q-component current reference i_q the controller output is added as shown in Figure 4. The third equation in the model (6) is rewritten.

$$C_{dc}\,\frac{dV_{dc}}{dt}+\frac{V_{dc}}{R_{dc}}=d_{nq}i_q \tag{10}$$

The three-phase filter currents are given by

$$\begin{matrix} i_{c1} \\ i_{c2} \\ i_{c3} \end{matrix} = \sqrt{\frac{2}{3}}\; i_q \begin{pmatrix} -\sin\theta \\ -\sin\left(\theta-\frac{2\pi}{3}\right) \\ -\sin\left(\theta-\frac{2\pi}{3}\right) \end{pmatrix} \tag{11}$$

The fundamental filter rms current I_c is

$$I_c=\frac{I_q}{\sqrt{3}} \tag{12}$$

The q-axis active filter voltage v_{Mq} is expressed as

$$v_{Mq}=q_{nq}v_{dc}=-z_{PF}I^{*}_{q1} \tag{13}$$

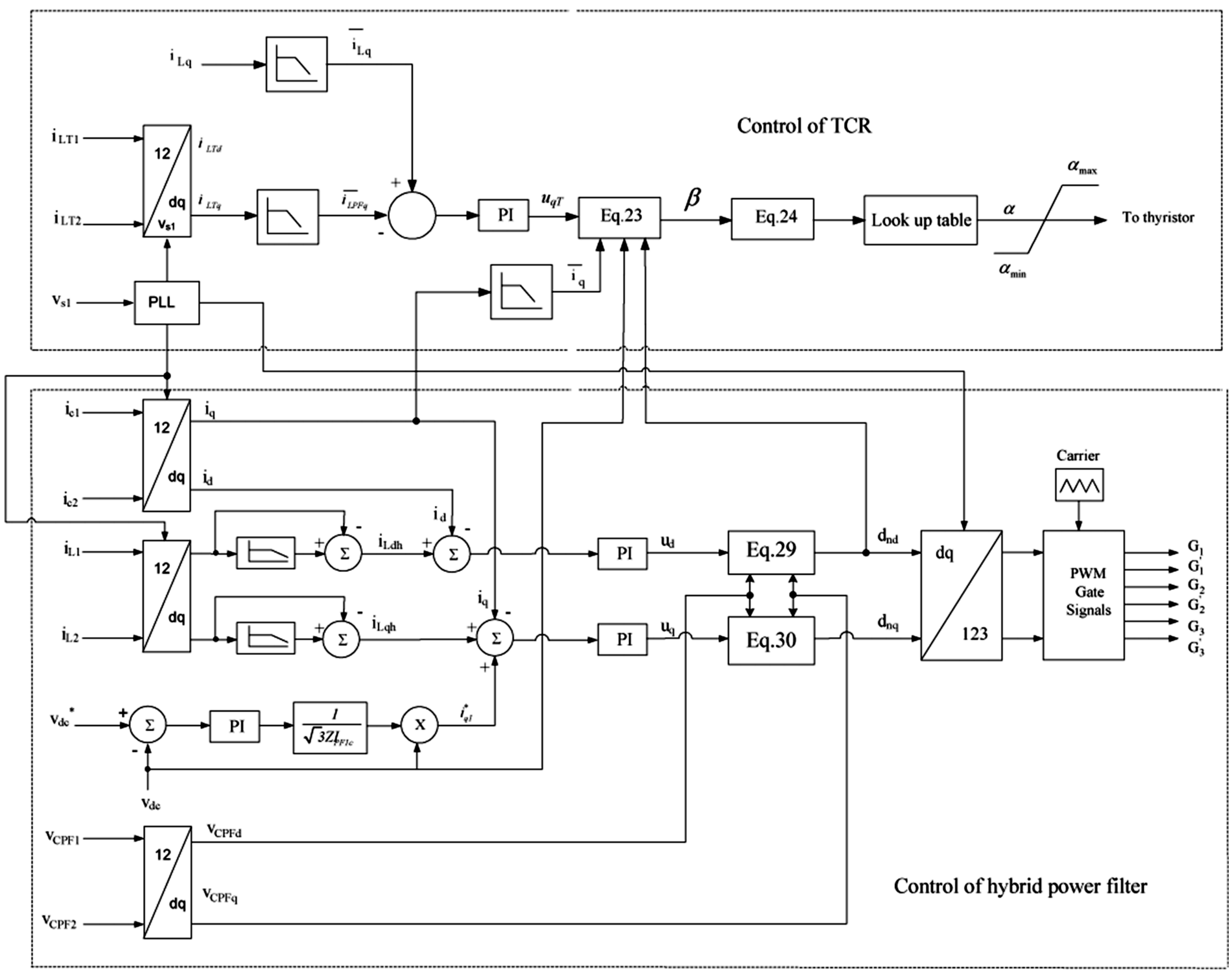

Figure 3: Control Scheme of the Proposed SHPF-TCR Compensator

Where Z_{PF1} is the impedance of the passive filter at 60 Hz and i^*_{q1} is a dc component.

An equivalent input u_{dc} is defined as

$$u_{dc} = q_{nq} i_q \tag{14}$$

The control effort of the dc voltage loop is deduced

$$I^*_{q1} = \frac{V_{dc}}{-Z_{PF1} I_q} u_{dc} \tag{15}$$

The dc component will force the SHPF-TCR compensator to generate or to draw a current at the fundamental frequency.

The response of the dc bus voltage loop is a second-order transfer function and has the following form:

$$\frac{V_d(s)}{V^*_d(s)} = 2\varepsilon\omega_{nv} \frac{s + \frac{\omega_{nv}}{2\varepsilon}}{s^2 + 2\varepsilon\omega_{nv} s + \omega^2_{nv}} \tag{16}$$

The closed-loop transfer function of dc bus voltage regulation is given as follows:

$$\frac{V_d(s)}{V^*_d(s)} = \frac{\frac{\sqrt{3}\, z_{PF1} k_p i_c}{V_{dc} c_{dc}} + \frac{\sqrt{3}\, z_{PF1} k_i i_c}{V_{dc} c_{dc}}}{s^2 + \frac{\sqrt{3}\, z_{PF1} k_p i_c}{V_{dc} c_{dc}} + \frac{\sqrt{3}\, z_{PF1} k_i i_c}{V_{dc} c_{dc}}} \tag{17}$$

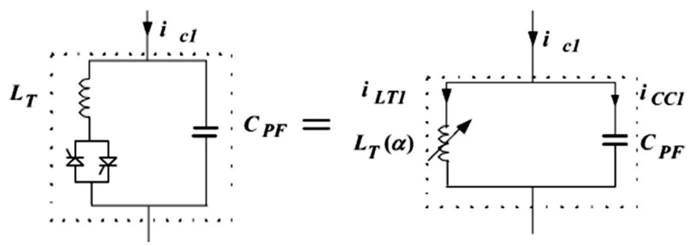

Figure 4: TCR equivalent circuit

5. MODELING OF TCR

Figure 4 shows the TCR equivalent circuit. Using Kirchhoff's voltage law, the following equations in 123 reference frame are obtained:

$$v_{s1} = L_T \frac{di_{LPF1}}{dt} + L_{PF} \frac{di_{c1}}{dt} + R_{PF} i_{c1} + d_{n1} V_{dc}$$

$$v_{s2} = L_T \frac{di_{LPF2}}{dt} + L_{PF} \frac{di_{c2}}{dt} + R_{PF} i_{c2} + d_{n2} V_{dc}$$

$$v_{s3} = L_T \frac{di_{LPF3}}{dt} + L_{PF} \frac{di_{c3}}{dt} + R_{PF} i_{c3} + d_{n3} V_{dc} \tag{18}$$

Applying Park's transformation, one obtains

$$L_T(\alpha) \frac{di_{LT_d}}{dt} = L_T(\alpha)\omega i_{LT_q} + L_{PF}\omega i_q - L_{PF} \frac{di_d}{dt} - R_{PF} i_d - d_{nd} V_{dc} + V_d$$

$$L_T(\alpha)\frac{di_{LT_q}}{dt} = -L_T(\alpha)\omega i_{LT_d} + L_{PF}\omega i_d - L_{PF}\frac{di_q}{dt} - R_{PF}i_q - d_{nq}V_{dc} + V_q \tag{19}$$

The reactive part is chosen to control the reactive current so that $v_q = 0$ and $L_P(\alpha)\omega i_{LT_d} = 0$

$$\frac{di_{LT_q}}{dt} = B(\alpha)\omega - L_{PF}\omega i_d - R_{PF}\frac{di_q}{dt} - R_{PF}i_d - d_{nq}V_{dc} \tag{20}$$

Where B(α) = 1/LF(α)ω is the susceptance. An equivalent input uqT is defined as

$$u_{qt} = \frac{di_{LT_q}}{dt} \tag{21}$$

According to this expression, one deduces

$$B(\alpha) = \frac{u_{qt}}{\omega - L_{PF}\omega i_d - L_{PF}\frac{di_q}{dt} - R_{PF}i_q - d_{nq}V_{dc}} \tag{22}$$

On the other hand, the equivalent inductance is given by

$$L_{PF}(\alpha) = L_{PF}\frac{\pi}{2\pi - 2\alpha + \sin(2\alpha)} \tag{23}$$

The susceptance is given by

$$B(\alpha) = B\frac{2\pi - 2\alpha + \sin(2\alpha)}{\pi} \tag{25}$$

6. MATLAB/SIMULINK RESULTS

Case 1: Performance of SHPF-TCR for harmonic generated load

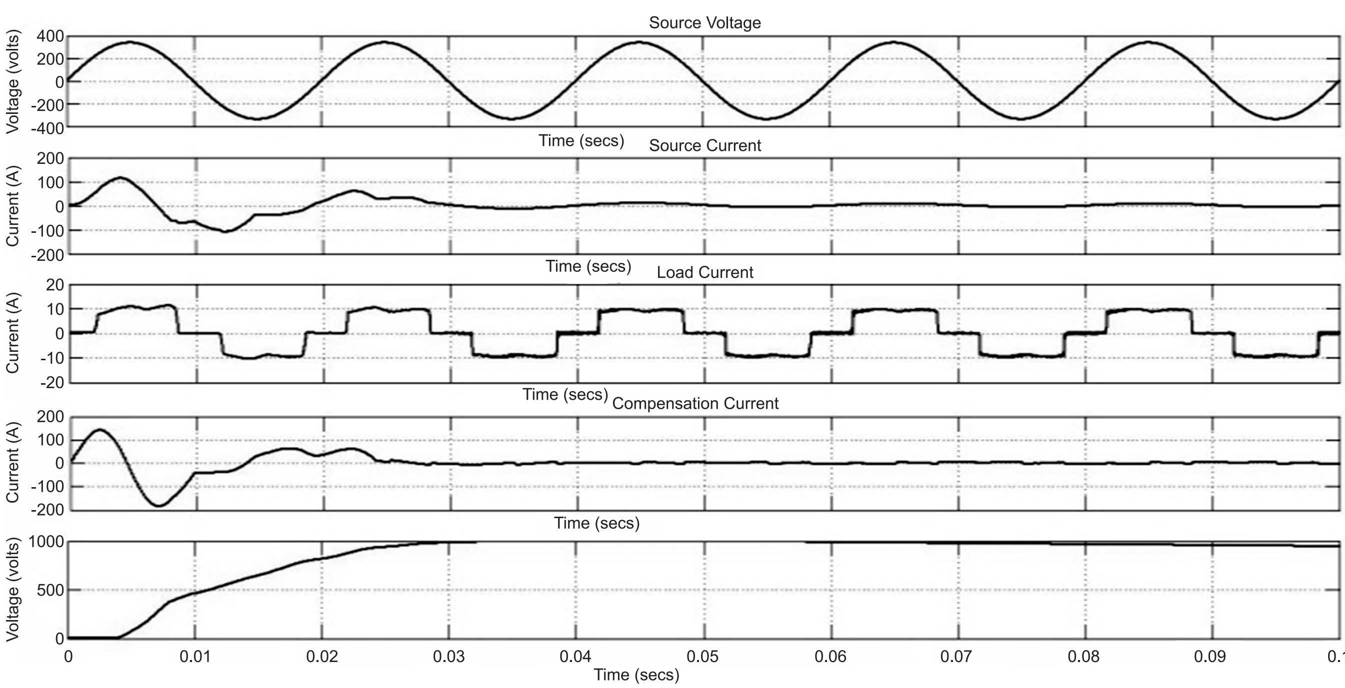

Figure 5: Simulation results for source voltage, source current, load current, compensation currents and dc link voltage

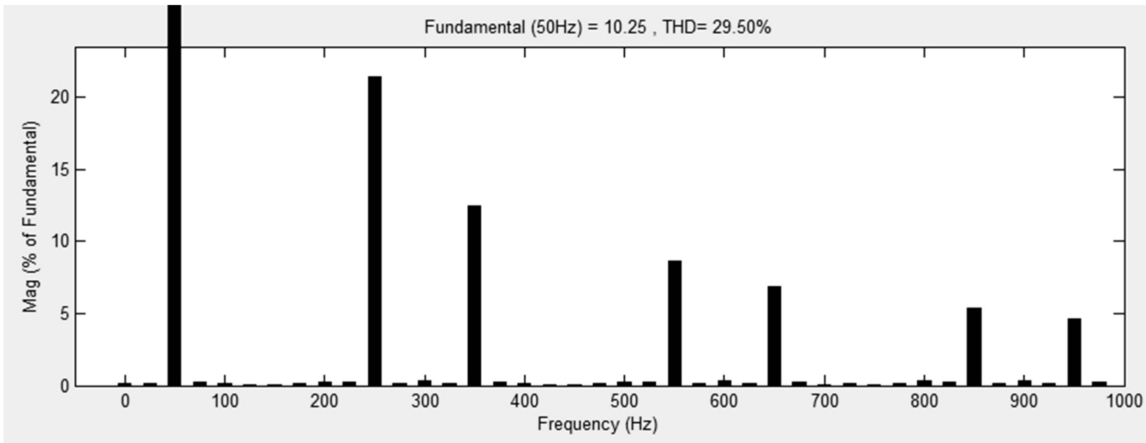

Figure 6: Harmonic spectrum for source current without compensation

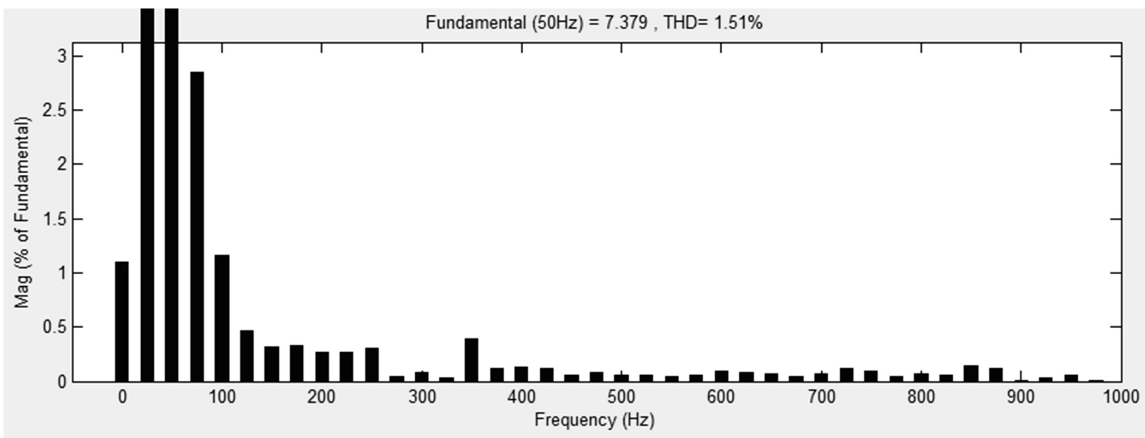

Figure 7: Harmonic spectrum for source current with compensation

Case 2: Performance of SHPF-TCR for distorted harmonic generated load

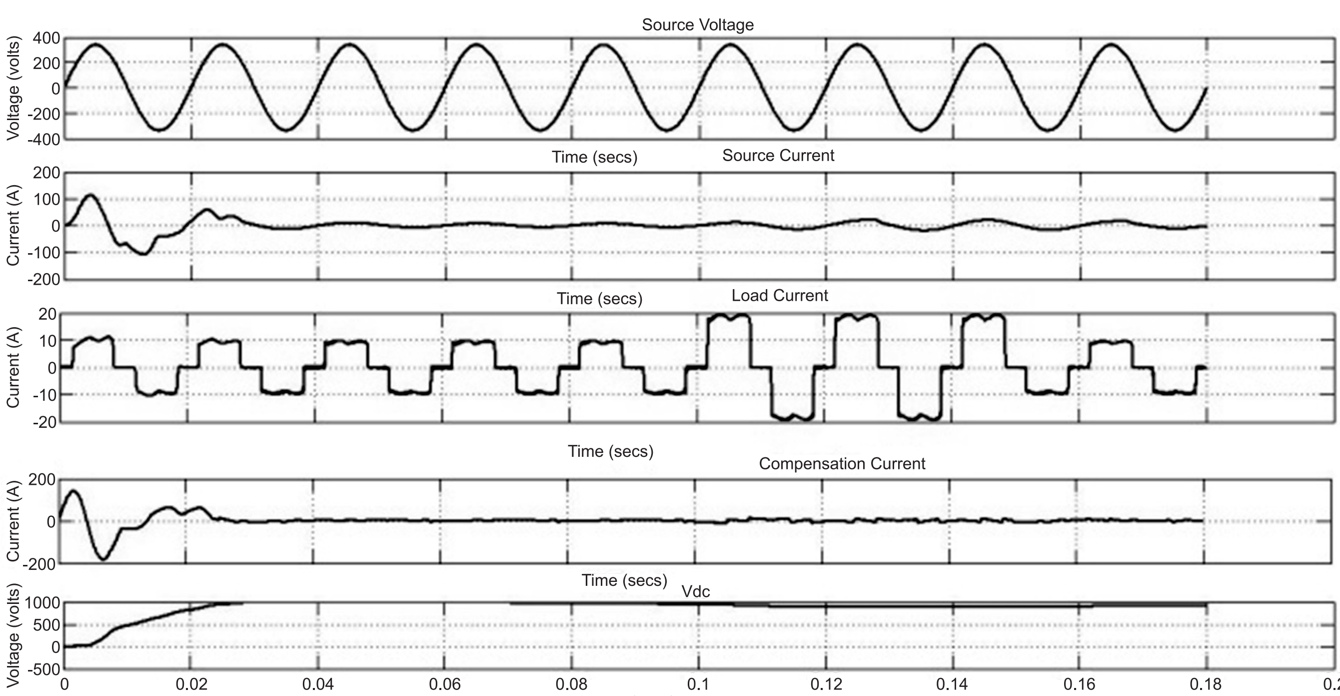

Figure 8: Source voltage, source current, load current, compensation currents and dc link voltage

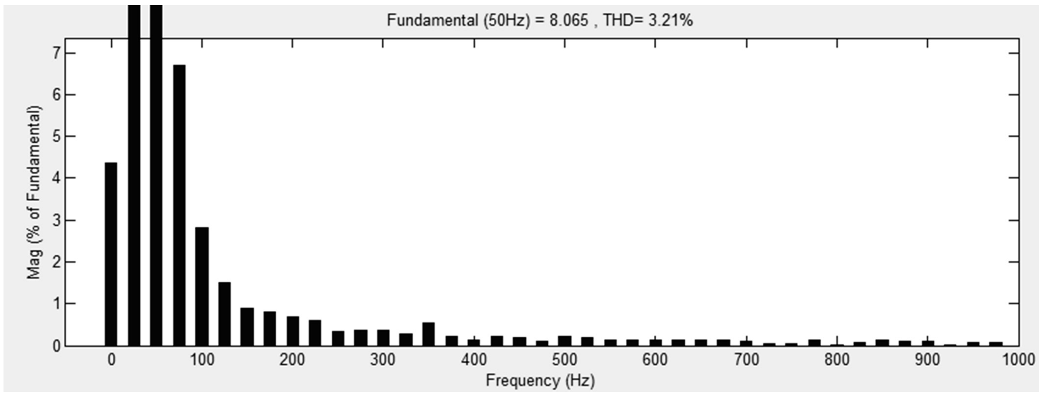

Figure 9: Harmonic spectrum for source current with compensation

Case 3: Performance of SHPF-TCR for harmonic and reactive type load.

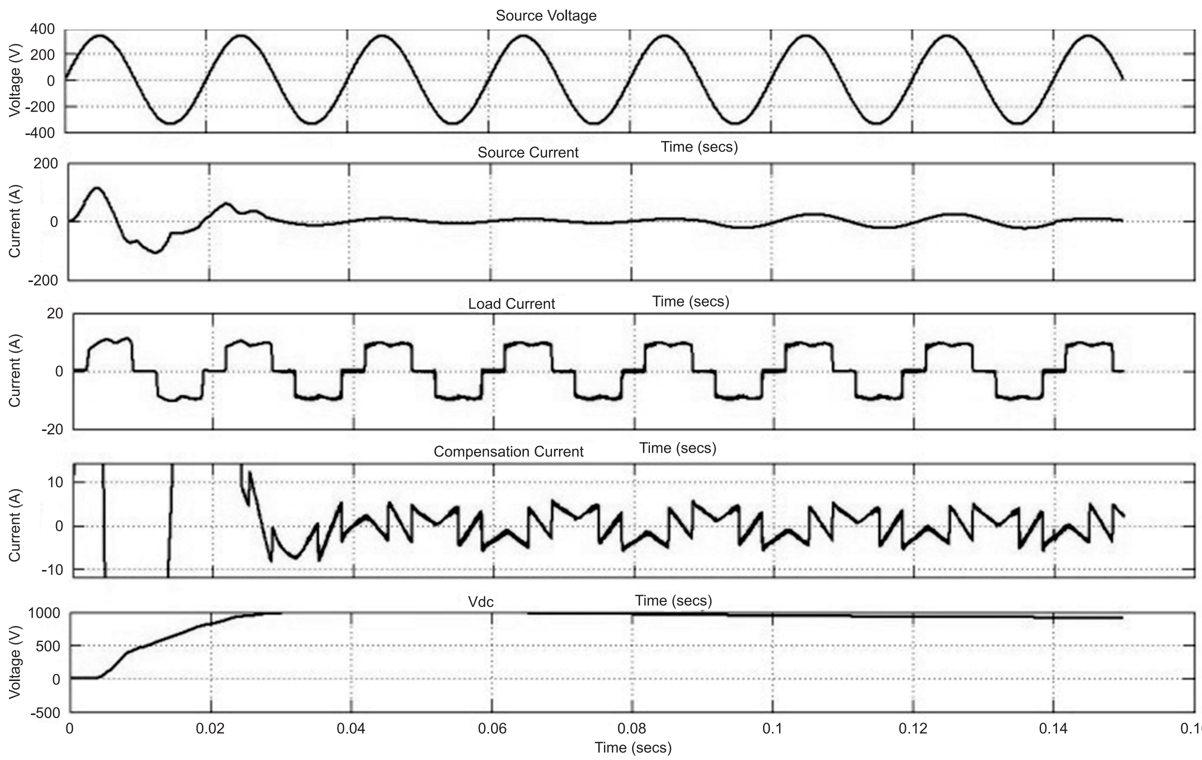

Figure 10: Simulation Results for Source Voltage, Source Current, Load Current, Compensation Currents and DC Link Voltage

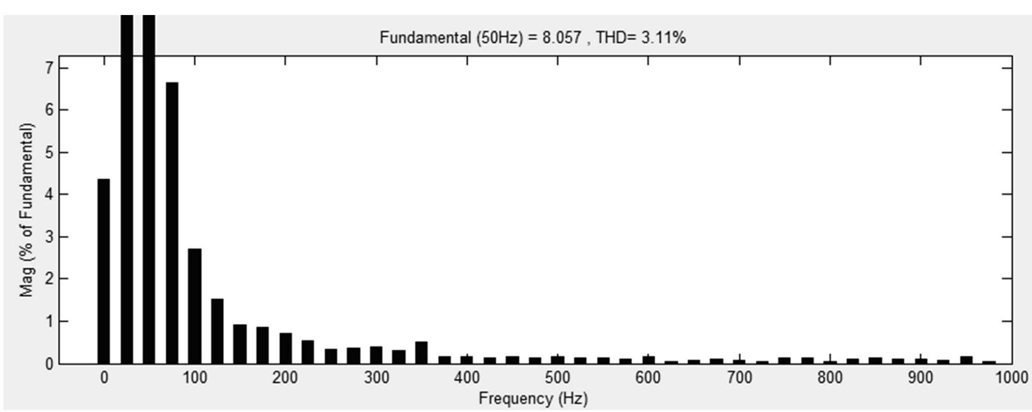

Figure 11: Harmonic spectrum for source current with compensation

Case 4: Performance of SHPF-TCR for harmonic generated load with fuzzy controller

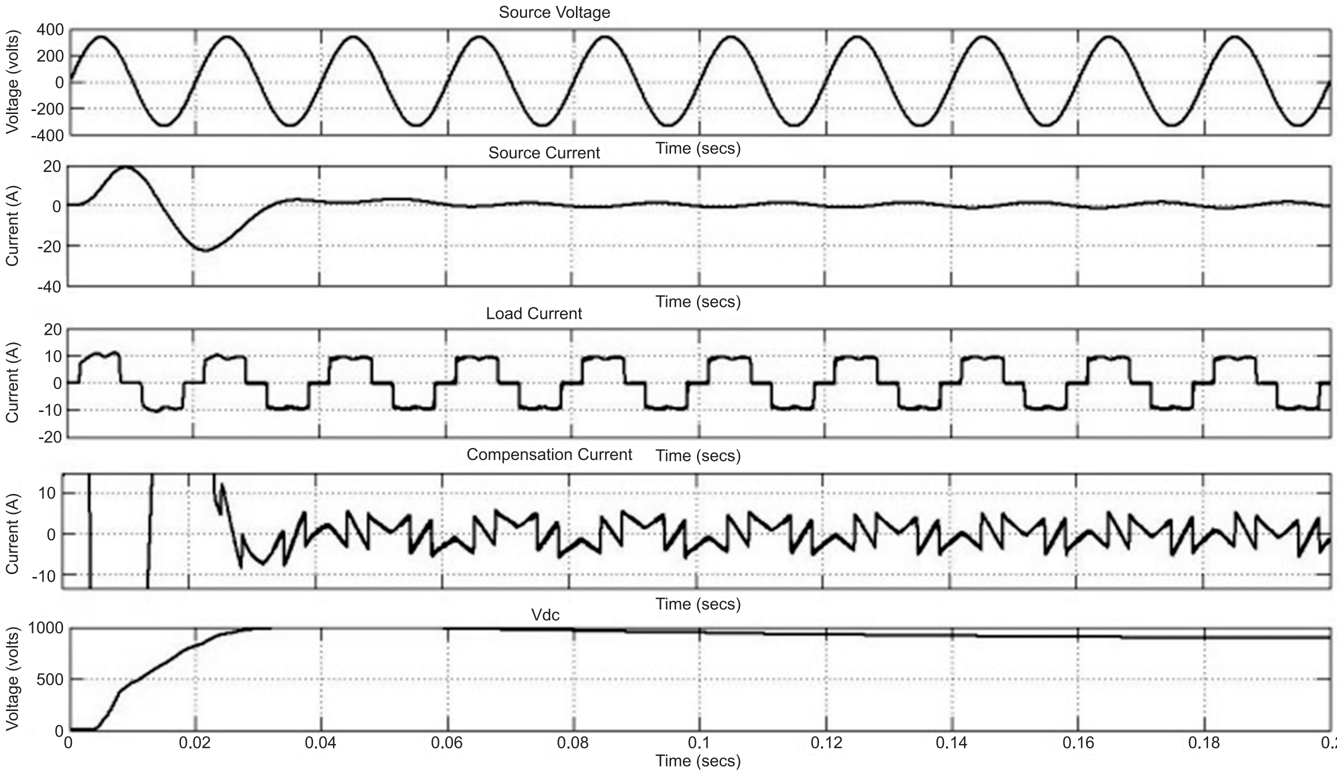

Figure 12: Simulation Results for Source Voltage, Source Current, Load Current, Compensation Currents and dc Link Voltage

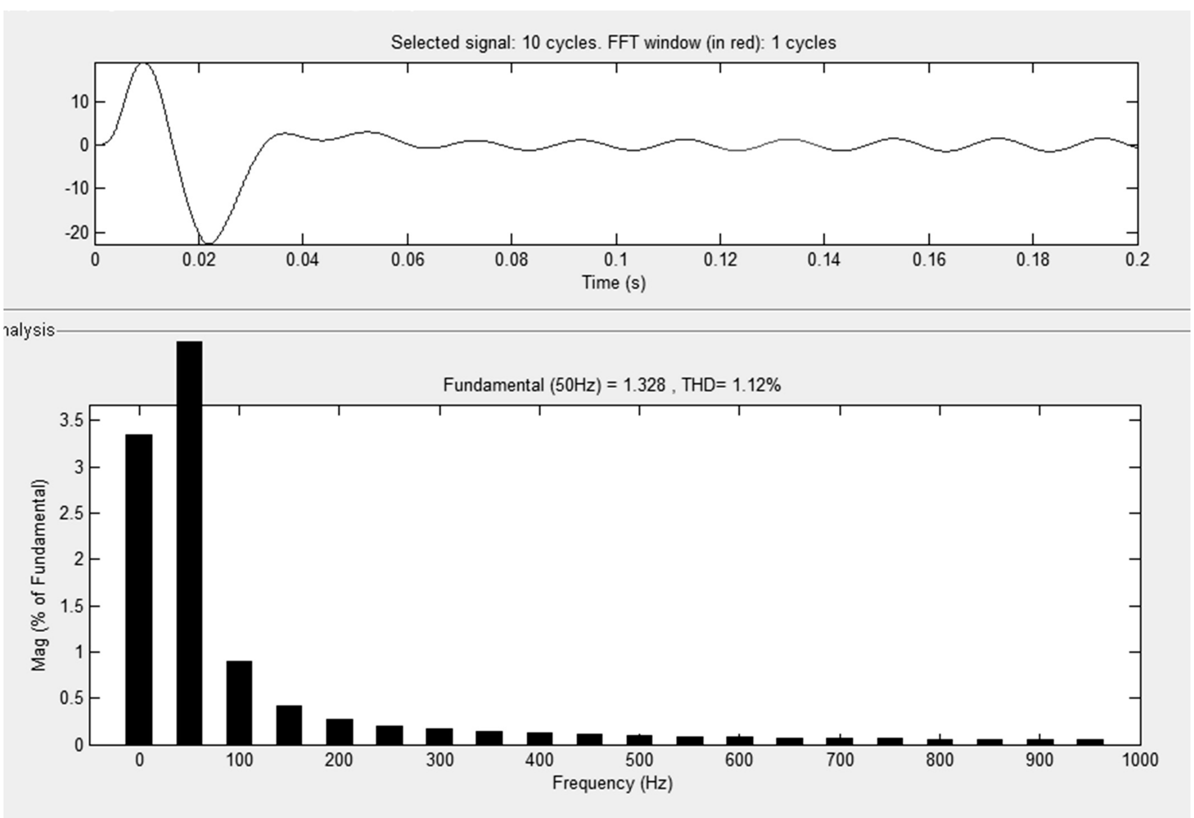

Figure 13: Harmonic Spectrum for Source Current with Compensation

7. %THD COMPARISON

	Case-1	*Case-2*	*Case-3*	*Case-4*
IEEE-519 and IEC 61000-3 harmonic standards	Less than 5%			
UPQC With Fuzzy	2.25% to 2.8% [15]			
SHPF and TCR with fuzzy	4.15%	3.21%	3.11%	1.12%

8. CONCLUSION

In this paper, TCR and SHPF's, SHPF-TCR compensator has been proposed to obtain reactive power compensation and harmonic elimination. For the active filter proposed model is to compensate the input voltage harmonics, and current harmonics caused by nonlinear load. To compensate the supply voltage and power quality issues such as harmonics, flicker, unbalance, sags, swells and for load current. Natural current and unbalanced with PI&fuzzy controller the APF is used in this paper so many shunt and TCR configurations have been discussed. And also according to IEEE-519 and IEC 61000-3 harmonic standards and UPQC with fuzzy is compared with proposed system. From this analysis the total harmonic distortion (THD) is reduced to 1.15%.

References

1. A. Hamadi, S. Rahmani, and K. Al-Haddad, "A hybrid passive filter configuration for VAR control and harmonic compensation," *IEEE Trans. Ind. Electron*., Vol. 57, No. 7, pp. 2419-2434, Jul. 2010.
2. P. Flores, J. Dixon, M. Ortuzar, R. Carmi, P. Barriuso, and L. Moran, "Static Var compensator and active power filter with power injection capability, using 27-level inverters and photovoltaic cells," *IEEE Trans. Ind. Electron*., Vol. 56, No. 1, pp. 130-138, Jan. 2009.
3. X. Wang, F. Zhuo, J. Li, L. Wang, and S. Ni, "Modeling and control of dual-stage high-power multifunctional PV system in d-q-0 coordinate," *IEEE Trans. Ind. Electron*., Vol. 60, No. 4, pp. 1556-1570, Apr. 2013.
4. J. A. Munoz, J. R. Espinoza, C. R. Baier, L. A. Moran, E. E. Espinosa, P. E. Melin, and D. G. Sbarbaro, "Design of a discrete-time linear control strategy for a multicell UPQC," *IEEE Trans. Ind. Electron*., Vol. 59, No. 10, pp. 3797-3807, Oct. 2012.
5. L. Junyi, P. Zanchetta, M. Degano, and E. Lavopa, "Control design and implementation for high performance shunt active filters in aircraft power grids," IEEE Trans. Ind. Electron., Vol. 59, No. 9, pp. 3604-3613, Sep. 2012.
6. Z. Chen, Y. Luo, and M. Chen, "Control and performance of a cascaded shunt active power filter for aircraft electric power system," *IEEE Trans. Ind. Electron*., Vol. 59, No. 9, pp. 3614-3623, Sep. 2012.
7. S. Rahmani, A. Hamadi, K. Al-Haddad, and A. I. Alolah, "A DSP-based implementation of an instantaneous current control for a three-phase shunt hybrid power filter," J. Math. Comput. Simul.—Model. Simul. Elect. Mach., Convert. Syst., Vol. 91, pp. 229-248, May 2013.
8. A. Hamadi, S. Rahmani, and K. Al-Haddad, "Digital control of hybrid power filter adopting nonlinear control approach," *IEEE Trans. Ind. Informat., to be published*.
9. A. Bhattacharya, C. Chakraborty, and S. Bhattacharya, "Parallelconnected shunt hybrid active power filters operating at different switching frequencies for improved performance," *IEEE Trans. Ind. Electron*., Vol. 59, No. 11, pp. 4007-4019, Nov. 2012.
10. S. Rahmani, A. Hamadi, N. Mendalek, and K. Al-Haddad, "A new control technique for three-phase shunt hybrid power filter," *IEEE Trans. Ind. Electron*., Vol. 56, No. 8, pp. 2904-2915, Aug. 2009.
11. A. Luo, X. Xu, L. Fang, H. Fang, J. Wu, and C. Wu, "Feedbackfeedforward PI-type iterative learning control strategy for hybrid active power filter with injection circuit," *IEEE Trans. Ind. Electron*., Vol. 57, No. 11, pp. 3767-3779, Nov. 2010.
12. M. I. Milanés-Montero, E. Romero-Cadaval, and F. Barrero-González, "Hybrid multiconverter conditioner topology for high-power applications," *IEEE Trans. Ind. Electron*., Vol. 58, No. 6, pp. 2283-2292, Jun. 2011.
13. A. Luo, S. Peng, C. Wu, J. Wu, and Z. Shuai, "Power electronic hybrid system for load balancing compensation and frequency-selective harmonic suppression," *IEEE Trans. Ind. Electron*., Vol. 59, No. 2, pp. 723-732, Feb. 2012.
14. A. Luo, Z. Shuai, W. Zhu, and Z. John Shen, "Combined system for harmonic suppression and reactive power compensation," *IEEE Trans. Ind. Electron*., Vol. 56, No. 2, pp. 418-428, Feb. 2009.
15. Y. Chen, XZha Wang, *Unified power quality conditioner (UPQC): The theory, modeling and application.* Power System Technology Power Con Int. Conf proc-2000*;* Vol. 3, p. 1329-1333.